Biologically Inspired CMOS Image Sensor for Fast Motion and Polarization Detection

Mukul Sarkar, *Member, IEEE*, David San Segundo Bello, *Member, IEEE*, Chris van Hoof, *Member, IEEE*, and Albert J. P. Theuwissen, *Fellow, IEEE*

***Abstract*— A complementary–metal–oxide semiconductor (CMOS) image sensor replicating the perception of vision in insects is presented for machine vision applications. The sensor is equipped with in-pixel analog and digital memories that allow in-pixel binarization in real time. The binary output of the pixel tries to replicate the flickering effect of an insect's eye to detect the smallest possible motion based on the change in state of each pixel. The pixel level optical flow generation reduces the need for digital hardware and simplifies the process of motion detection. A built-in counter counts the changes in states for each row to estimate the direction of the motion. The designed image sensor can also sense polarization information in real time using a metallic wire grid micropolarizer. An extinction ratio of 7.7 is achieved. The 1-D binary optical flow is shown to vary with the polarization angle of the incoming light ray. The image sensor consists of an array of 128 × 128 pixels, occupies an area of 5 × 4 mm^2 and it is designed and fabricated in a 180-nm CMOS process.**

***Index Terms*— Analog and digital polarization, collision detection, image sensor, motion detection, optical flow, polarization, wire grid polarizer.**

I. Introduction

OBJECTS become visible through many different phenomena of light e.g. reflection, refraction. The way in which creatures see differs in regard to their shape, perception, colour visualization, resolution and their depth perception. Eyes can be simply defined as organs or visual systems for spatial and temporal vision. High resolution spatial vision can be achieved by increasing the number of photoreceptors in the visual system, as in the single chambered human eye. High temporal resolution can be obtained by multiplying the visual system in its entirety, similar to the compound eyes in insects. The single chambered human eye is a single lens vision system and produces very high resolution images. However the temporal resolution is limited and thus humans have low sensitivity to motion. The image resolution of the compound eyes is very poor but they have very high sensitivity to motion due to their high temporal resolution. The vision processing in compound eye is also relatively simple compared to the single aperture human eye.

Biological vision systems are a source of inspiration in the development of small autonomous vision sensors. The compound eyes of insects are known to process visual information efficiently and are able to detect fast motion in a visual scene. They are thus good examples of low power vision systems. The compound eyes, besides performing their function in forming images and motion detection, are also sensitive to other properties of light, *i.e.* the wavelengths and vector of skylight polarization. Human eyes are, on the other hand, polarization blind.

Polarization provides additional visual information to intensity and wavelength, and provides a more general description of light. Therefore, polarization provides richer sets of descriptive physical constraints for the interpretation of the imaged scene. For example, polarization information can be used for material classification. Information on the type of material can provide important information about the scene in machine vision applications. An external polarization filter is usually coupled to a CCD or a CMOS image sensor and the nature of the transmitted irradiance after reflection helps in classifying materials. The disadvantage of such a system is that the linear polarization filters have to be externally controlled, which prevents the miniaturization of optical sensors for material classification. For real-time polarization vision, the linear micropolarizers with varying orientations are being monolithically integrated directly over the photodiodes. Micropolarizers have been fabricated with metal grids [1], [2] and organic materials [3].

Besides the polarization detection ability, the insects' eyes are also good in detecting motion in a visual scene. This helps them in, for example, avoiding collision with obstacles, using low level image processing and with little computational power. Reliable estimation of the time to collision between two moving objects is very important in many applications such as autonomous agent navigation or predictive crash sensors for autonomous safety systems. Currently existing non-biologically inspired motion detection systems use a CCD/CMOS camera and digital processing devices to detect the moving object. These are computationally intensive and are thus not suitable for low-power real-time implementation.

Manuscript received May 17, 2012; revised November 11, 2012; accepted December 2, 2012. Date of publication December 13, 2012; date of current version January 29, 2013. The associate editor coordinating the review of this paper and approving it for publication was Dr. Gert Cauwenberghs.

M. Sarkar was with IMEC, Eindhoven 5656 AE, The Netherlands, and also with the Electronic Instrumentation Laboratory, Delft University of Technology, 2628 CD Delft, The Netherlands. He is now with the Indian Institute of Technology Delhi, New Delhi 110016, India (e-mail: msarkar@ee.iitd.ac.in).

D. S. S. Bello and C. van Hoof are with IMEC, Leuven 3001, Belgium (e-mail: David.SanSegundoBello@imec.be; Chris.VanHoof@imec.be).

A. J. P. Theuwissen is with Harvest Imaging, Bree 3960, Belgium, and also with the Electronic Instrumentation Laboratory, Delft University of Technology, CD Delft 2628, The Netherlands (e-mail: a.j.p.theuwissen@tudelft.nl).

Color versions of one or more of the figures in this paper are available online at http://ieeexplore.ieee.org.

Digital Object Identifier 10.1109/JSEN.2012.2234101

For real-time motion detection, analog VLSI chips employing early vision processing of the visual scene are becoming popular [4], [5]. They employ simple, low accuracy operations at each pixel for each image or for a sequence of images, resulting in a low-level description of a scene useful for higher level machine vision applications. Pixel level processing helps in decreasing the data rate from the sensor, compared to frame level processing. This often results in compact, high speed and low power solutions. Focal plane computations are also free from temporal aliasing, which is usually a problem in motion detection algorithms.

Temporal contrast is necessary for all motion vision algorithms to work. Polarization contrast is the basis for motion detection in certain animals, such as the crayfish [6]. In crayfish, the polarization vision supports motion vision under circumstances in which intensity contrast is minimal or absent. In a low contrast environment, the polarization sensitivity enhances the contrast and thus contributes to motion detection. To detect the temporal change of the e-vector distribution, crayfish use antagonistic inputs from orthogonally oriented polarization analyzers. In machine vision applications where the contrast is low, the motion detection using polarization vision can be very useful.

This paper presents a CMOS image sensor with real time polarization sensing ability using a metallic wire grid formed with CMOS metal layers. The ability of the sensor to detect polarization is shown. One-dimensional binary optical flow is used to represent polarization information in digital format. The binary optical flow is shown to have an angular dependence on the angle of the linear polarizer. The "flickering effect" of the insects eye is replicated using the binary optical flow to detect fast motion. The binary images are used to speed up low level motion detection with low complexity and power consumption. These algorithms are based on pixel changes instead of full image processing and thus improve performance.

Section II briefly presents the theory behind motion detection using optical flow. Section III describes the designed image sensor to detect polarization and to generate binary one-dimensional optical flow. Section IV and V presents the experimental results pertaining to polarization representation and motion detection respectively. Conclusions are presented in Section VI.

II. Theory - Motion Detection

Motion is usually determined from image sequences. The spatiotemporal image sequences can be represented using the plenoptic function [7]. For a pinhole camera, the plenoptic function can be written as

$$\mathrm{P} = \mathrm{P}\,(\mathrm{x}, \mathrm{y}, \mathrm{t}, \lambda) \tag{1}$$

where x, y are the spatial coordinates in the image plane, λ is the wavelength of light, and t is the time. From equation (1) the motion constraint equation can be derived which relates the image velocity to the spatiotemporal derivates of the image at a particular location [7].

$$\mathrm{I_x u + I_y v + I_t} = 0 \tag{2}$$

where $u(x, y, t)$ and $v(x, y, t)$ are the horizontal and vertical components of the motion respectively and I_x, I_y and I_t are the derivatives of the image (x, y, t) in the corresponding directions.

Based on the variation in the intensity obtained from the projection of the plenoptic function on the image sensors from the moving object, three conventional approaches are used to detect motion: temporal differencing [8]; background subtraction [9]; and optical flow [10].

Temporal differencing attempts to detect moving regions by making use of the differences between two consecutive frames (two or three) in a video sequence. This method is highly adaptive to dynamic environments, but is poor in detecting certain types of moving objects [11]. Background subtraction compares the current image with the reference image to separate the background and foreground [12]. The background subtraction method requires both the background scene and the camera to be stationary. This method is extremely sensitive to dynamic scene changes, due to background illumination changes. When the optical scene or the camera is in motion, optical flow is the most used method. Optical flow is the pattern of apparent motion of objects, surfaces, and edges in a visual scene caused by the relative motion between an observer and the scene. Insects are also known to use optical flow to detect obstacles in their flying path.

Optical flow estimation methods can be classified into three main groups: differential methods; matching-based methods and frequency/phase-based. In differential methods, the velocity is obtained by dividing the temporal derivate of local luminance by its spatial derivative. They are highly susceptible to errors under noisy conditions and are thus not preferred in low signal-to-noise ratio regimes [13]. Matching based methods or correlation based methods usually use techniques to either maximize cross-correlation or minimize differential errors. They are robust to large motion and brightness variations, however it is difficult to estimate sub-pixel displacements [14]. Frequency/phase based methods use local energy or phase information to determine the velocity of the moving object. However the output is limited by the design of the filter used and these methods are also susceptible to noise [14].

In biological vision, the correlation based model is often used to account for motion [15]. The most popular bio-inspired correlation-type elementary motion detector (EMD) was first proposed by Hassenstein and Reichardt [16]. This model is very well established and often used in bio-inspired robots [17], [18]. The EMD correlates the response of one photoreceptor to the delayed response (inhibitory response) of an adjacent photoreceptor, both looking in the same direction. The transient response obtained by subtracting the two images is sensitive to temporal changes in the intensity of light and thus is relevant in motion detection of the objects. To retrieve the distance of the obstacle information, the optical flow from different regions of the visual field needs to be spatially integrated. Existing implementations of the EMD use a complex circuit with many active and passive components in order to obtain the inhibition of the signal and the correlation.

In order to have compact and low-power biologically inspired systems, the estimation of the optical flow has to

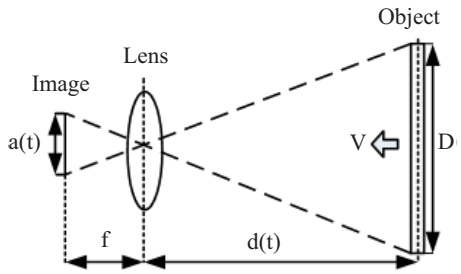

Fig. 1. Perception of approaching objects.

be simplified. The collision avoidance maneuvers of insects can be explained in terms of perception of looming stimuli or expanding images. To understand the plenoptic function of expansion of images the motion constraint equation (2) is used. Since in collision detection the motion is assumed to be only in the vertical direction of the focal plane, the motion constraint equation can be rewritten as

$$I_y v + I_t = 0\,. \tag{3}$$

Equation (3) shows that the time of impact or time of collision of the object is directly proportional to the velocity of the object. Equation (3) can be better understood using figure 1, which shows an image of an approaching object of diameter D at a constant velocity V along the optical axis. The distance between the lens and the object is $d(t)$ while the focal length of the lens is f.

The diameter of the obtained image with respect to time is given as:

$$a\,(t) = \frac{f \times D}{d\,(t)}\,. \tag{4}$$

The size image $a(t)$ in equation (4) increases with a decreasing distance $d(t)$ and vice versa. The change in the image size affects the optical flow perceived by the image sensor. This setup can also be used for horizontal motion detection.

III. Sensor Description

The designed sensor is described in [7]. The image sensor consists of an array of 128 by 128 pixels, it occupies an area of 5 × 4 mm^2 and it has been designed and fabricated in the 180nm CMOS CIS process from UMC.

A. Sensor for Polarization Detection

The sensor has an embedded linear wire grid polarizer in each pixel, realized with the first metal layer of the process on top of a pinned photodiode (p^+/n^-/p-sub) [7]. The linear wire grid polarizer was implemented using thin metal strips with a line/space of 240 nm/240 nm (pitch of 480 nm) as shown in figure 2. Normally, such a wire grid structure would function as a simple diffraction grating, but when the pitch or period of the wires is less than half the wavelength of the incoming light, it becomes a polarizer.

The array of 128 by 128 pixels was split into three regions as shown in figure 3:

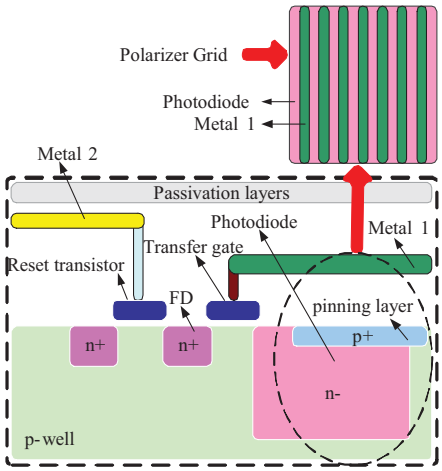

Fig. 2. Wire grid Polarizer.

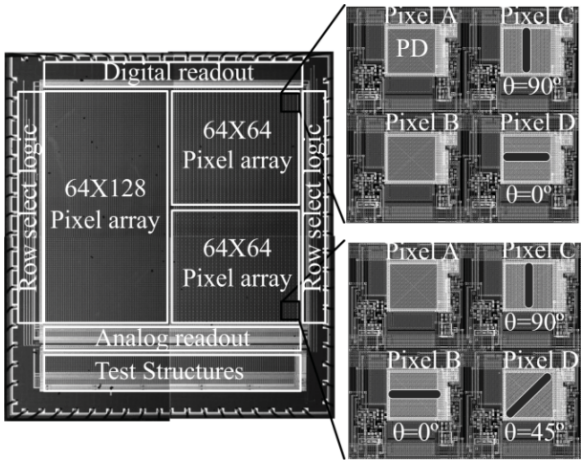

Fig. 3. Sensor regions with different polarizing angles.

1) A 64 × 128 array without a metal grid used for normal imaging applications
2) A 64 × 64 array (sense region 1) consisting of 2 by 2 pixel arrays where two pixels (A and B) measure the intensity while the other two measure the 0° (D), and 90° (C) polarized intensity, respectively
3) A 64 × 64 array (sense region 2) consisting of 2 by 2 pixel arrays where one pixel records the intensity of the light (A) while the other 3 record the 0° (B), 45° (C) and 90° (D) polarized intensity.

B. Sensor for Motion Detection

Each pixel of the designed image sensor (figure 3), contains a pinned photodiode, an analog comparator, two banks of analog memories and two SRAMs for digital memory. A simplified pixel diagram is shown in figure 4.

The image capture begins with a reset of the pixel by closing the *RST* switch. The voltage at the floating diffusion node (*FD*) is then set to the reset voltage V_{rbias}. After opening the reset switch, the photodiode starts accumulating the photo-generated charge. The time spent accumulating charge is referred to as integration time. At the end of the integration time, the accumulated charge is transferred to the *FD* node.

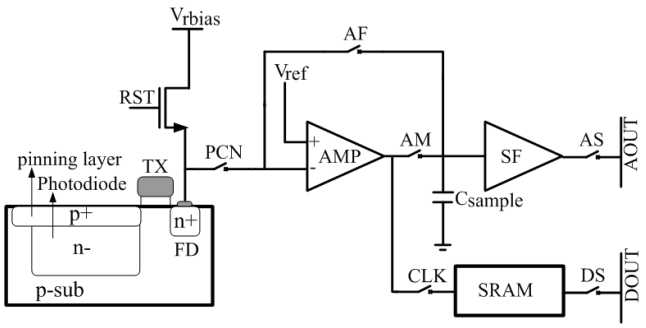

Fig. 4. Simplified pixel architecture.

The voltage change at the *FD* node capacitance due to the transferred photo-charge is sampled onto one of the two available sampling capacitors C_{sample}, when the switch *AM* is closed. The source follower *SF* loads the column bus *AOUT* via the analog row selection switch *AS* with the signal sampled on the sampling capacitor during readout of the pixel.

After the image is captured, the photodiode is disconnected from the processing elements using the switch *PCN*. The analog signal on C_{sample} is compared with a reference voltage V_{ref}, by using the amplifier *AMP* as a comparator. The comparator in the pixel is used to detect the difference between the integrated charge from the photodiode and an external threshold voltage. This allows the generation of binary optical flow similar to the effect of "flickering" in insects' eyes. The resulting binary data is stored in the *SRAM* cell when the switch *CLK* is closed. Two such *SRAM* cells are available to store the binary data of the two sampling capacitors. The switch *DS* loads the column bus *DOUT* with the binary value stored in the *SRAM* cell. The streaming binary data in the column bus, is spatially integrated by a row-wise 7-bit counter (figure 5). The counter counts the number of active high pixels in each row. From the digital images, the percentage of active high pixels for a given illumination condition which is given by the ratio of total active high pixel to the total number of pixels in the array can be computed as:

$$\%\ \text{of active high pixels} = \frac{\text{Total active high pixels}}{\text{Total number of pixels}}. \qquad (5)$$

Equation (5) represents the spatially integrated one-dimensional binary optical flow. The percentage of the active high pixels will increase with the approaching object as predicted by equation (4).

IV. Analysis - Polarization Detection

When randomly polarized light is transmitted through an ideal wire-grid polarizer, the electromagnetic fields orthogonal to the wires will be transmitted and the electromagnetic fields parallel to the wire will be reflected. The transmitted irradiance follows the "law of Malus" which states that the maximum transmitted intensity is a cosine function of the transmission axis of the polarization filter. Linear polarizers are characterized by the transmittance efficiency and the extinction ratio. The *transmittance efficiency* is the fraction of the total incident light that is transmitted through the linear polarizer.

TABLE I
Performance Comparison of the Available Polarization Sensors

	[20]	[21]	[1]	This Work
Imager type	CCD	CMOS	CMOS	CMOS
Polarizer type	Aluminum nanowires	Micro-patterning metal wire polarizer	Standard CMOS metal layers	Standard CMOS metal layers
Spatial orientations	0°, 45°, 90° & 135°	0°, 90° and right handed circular polarized	0° & 90°	0°, 45° & 90°
Array size	1000 × 1000	-	30 × 30	64 × 64
Pixel pitch	7.4 μm	5 μm	20 μm	25 μm
Grating thickness	0.14 μm	5 μm	-	0.35 μm
Grating width	0.75 μm	-	0.6 μm	0.24 μm
Grating pitch	0.14 μm	-	1.2 μm	0.48
Extinction ratio	$\sim$ 60 (λ = 530 nm)	$\sim$ 1100 (λ = 500 nm)	2.3 (λ = 633 nm)	6.6 & 7.7 (λ = 550 nm)

The *extinction ratio* (ER) is a measure of the polarization contrast of a linear polarizer and it is defined as the ratio between the maximum and minimum transmitted irradiances through the linear polarizer.

A. Analog Polarization Detection

In order to characterize the polarization behavior of the sensor, a polarized light is obtained by passing an unpolarized light from a DC light source through a linear polarizer. The transmission axis of the external linear polarizer is varied from 0° to 180° in steps of 15° to change the polarization angle of the light reaching the image sensor. The normalized analog output of the pixels sensitive to 0°, 45° and 90° for varying transmission axis of the external linear polarizer has already been presented in [19] and is shown in figure 6.

For 0° polarization the maximum transmittance obtained was 38.4% while the minimum transmittance was 5.45%. For 90° polarization the maximum transmittance observed was 42.4% while the minimum transmittance observed was 0.6%. The calculated extinction ratio for the linear polarizer is 7.7. A performance comparison of the designed polarization sensor with the available wire-grid polarizers in literature is shown in Table I.

B. Digital Polarization Detection

The analog polarization information needs additional processing for inference and is not suitable for real time applications. The digital polarization sensing principle is that of computing and analyzing the one-dimensional correlational optical flow from the intensity variations generated by a moving object on the sensor focal plane. The one-dimensional binary optical flow is represented by the percentage of active pixels in a pixel array at a fixed time.

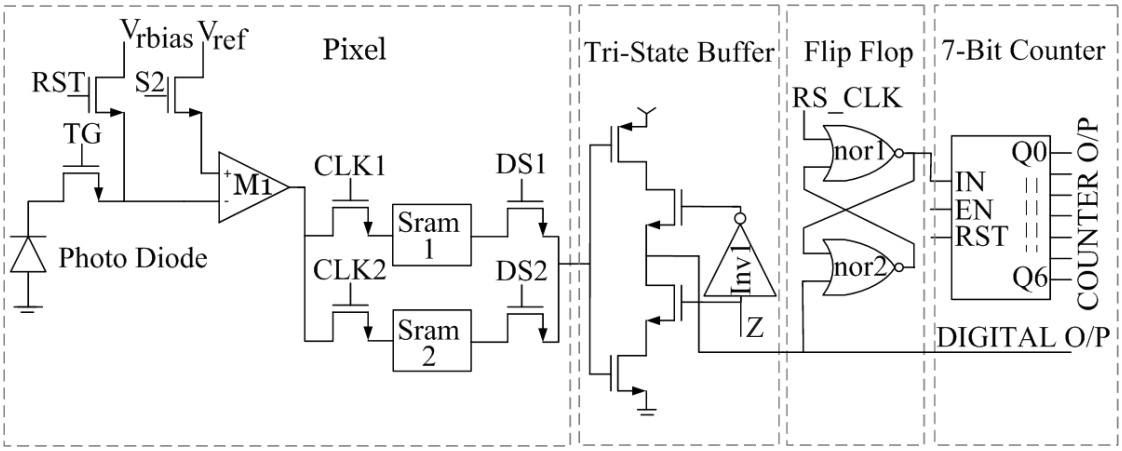

Fig. 5. Digital signal chain.

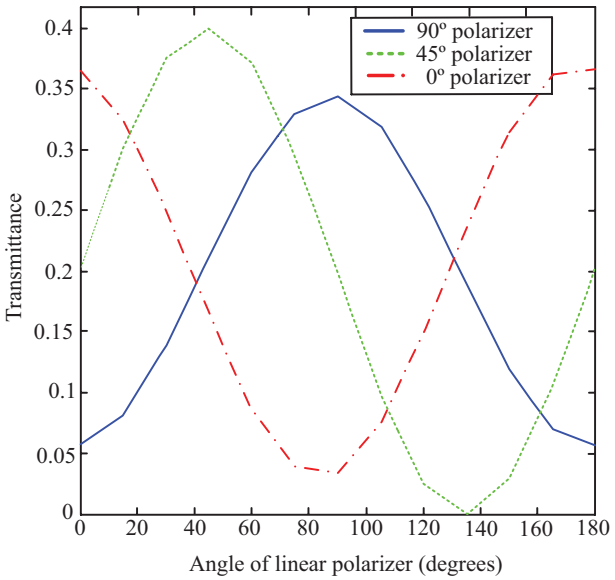

Fig. 6. 0°, 90°, and 45° polarization profiles in polarization sense region 2.

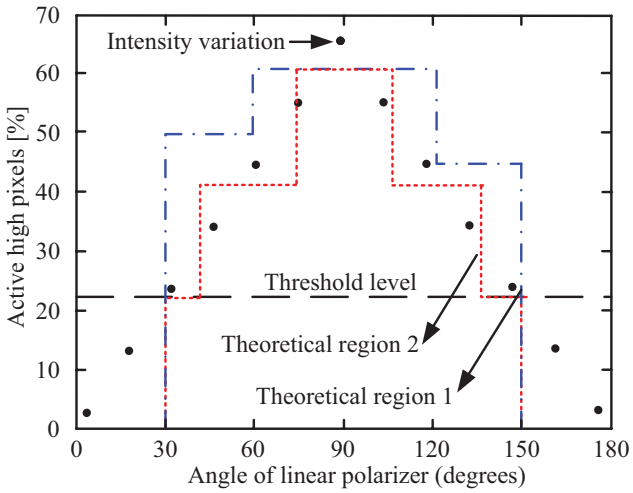

Fig. 7. Theoretical behavior of one-dimensional optical flow with variation in linear polarizer angle.

The expected theoretical behaviour of the one-dimensional binary optical flow for the two polarization sense regions (figure 3) is shown in figure 7. For the polarization sense region 1, when the object is moving towards the imaging plane the intensity of the pixels slowly increases. As the light intensity reaches the threshold level, the two intensity sensitive pixels store a digital "1", the output of the comparator, in the *SRAM* cells. The percentage of active high pixels shows a step rise to around 50%. As the intensity is further increased around 90°, the 90° sensitive pixels will slowly start to have a have a digital "1", as their comparators' outputs, and hence the percentage of active high pixels will increase above 50%. Ideally, when all the 90° sensitive pixels turn high, 75% of the pixels in region 1 will be active high. However due to the attenuation of the light by the external polarizer not all 90° sensitive pixels turn high. In the polarization sense region 2, the theoretical behavior of the percentage of active high pixels would be the same as region 1, except that as the intensity increases, the 45° sensitive pixels start to turn high. Thus there is an additional step rise when the polarizer angle is 45°. In the experiments, the optical flow is obtained by increasing the light spot gradually from the center to the periphery of the polarization sense regions, using a linear polarizer. This results in a linear increase in the percentage of active high pixels with the variations in the linear polarizer angle, instead of the expected step rise.

The analog performance for the 90° polarizer filter in the two polarization sense regions 1 and 2 is compared with the one-dimensional binary optical flow for varying angle of linear polarizer in figure 8. The measured one-dimensional binary optical flow is shown to have an angular dependence on the angle of the linear polarizer and is very similar to the theoretically predicted behavior. The optical flow and analog representations of polarization in region 2 match closely. It can be predicted that by increasing the number of metallic wire grid orientations over the photodiode a digital representation of polarization very similar to the analog representation can be obtained [22].

A generalized algorithm to represent polarization information in digital form will have multiple advantages in low

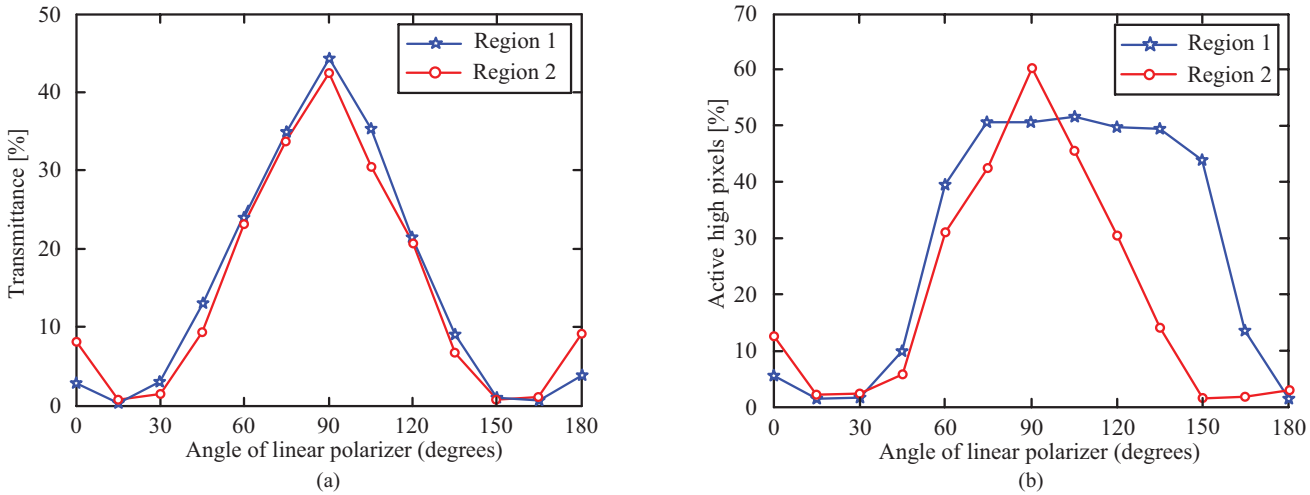

Fig. 8. 90° polarization in sense regions 1 and 2. (a) Analog and (b) digital (optical flow variation).

Fig. 9. Perception of approaching objects.

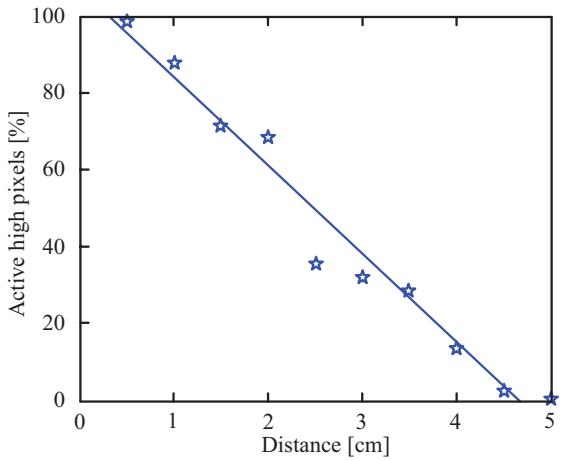

Fig. 10. 1-D binary optical flow variation with approaching object.

level polarization based machine vision applications. Based on the one-dimensional binary optical flow variations with the polarization angle, the degree of polarization and polarization Fresnel ratio can be formulated in binary format which will allow focal plane processing of applications like material classification and autonomous agent navigation. These applications using analog polarization information are presented in [7]. Such a sensor would be small, with a low data rate and low power consumption, which are required characteristics in future generations of sensors in machine vision applications.

V. Analysis - Motion Detection

Motion can either be in a horizontal direction or in a vertical direction. As mentioned in section II, motion detection has been predominantly done using temporal difference computation algorithms, wherein two consecutive images are used to detect motion in the scene. Motion detection using a synchronous event-based temporal contrast vision sensor was proposed by [23], [24], wherein the intensity information is continuously quantized into binary events. The real-time motions of the object are converted into binary events and asynchronously delivered to the outside using an address-event-representation (AER) protocol [25]. In this section we describe motion detection using optical flow, similar to the "flickering effect" in the insects' eyes. To simplify the optical flow generation algorithm, the binary output of the pixel is used as explained in Section III.

A. Motion Detection in Vertical Direction - Collision Detection

Vertical motion of an object towards the sensor leads to a collision and thus needs to be prevented. In the collision detection experiments, the image sensor is held stationary so that the optical flow is always generated by the motion of the object in the visual field. Figure 9 shows the variation in the light spot (approaching object). As the object moves closer to the image sensor, the image size (spot size on the imaging plane) grows or the optical flow expands. With the expansion of the optical flow the intensity profile of the pixel will also increase, and more pixels will have an output voltage higher than the reference voltage, and a digital "1" will be stored in the *SRAM* cells in figure 5.

The variation in the percentage of active high pixels with the variation in the distance of the light source for single image capture is shown in figure 10. It shows that when the light source approaches the image sensor, the optical flow causes more pixels to become active thus increasing the percentage of active high pixels.

One of the major requirements of motion detection using correlation models is temporal decorrelation. Temporal

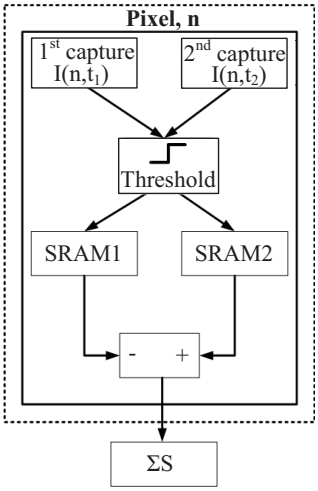

Fig. 11. Modified EMD model for collision detection.

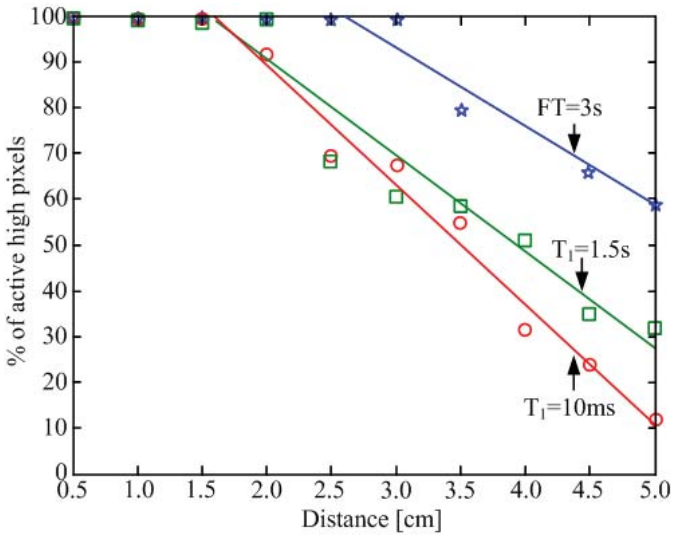

Fig. 12. Temporally decorrelated optical flow with approaching objects.

decorrelation can be obtained using differential imaging, where two samples are spaced in time. The differential image is generated using partial charge transfer, where the integrated charge at the photodiode capacitance is transferred to the *FD* node multiple times in one frame (possible due to the two analog memories available in the pixel). Figure 11 shows the algorithm used. The first image capture is at a time instance of T_1 and the second capture is at T_2. The captured samples are then compared with the reference voltage and the digital output is stored in the two *SRAM* cells available in the pixel. The differential image of the two spatially integrated digital images obtained from *SRAM1* and *SRAM2* was computed off chip for this version of the sensor.

The temporal decorrelation of the optical flow obtained using the partial charge transfer is shown in figure 12. The figure shows the variation in the percentage of active high pixels of two image captures for varying distance of the object from the imager. The first image is captured after an integration time of T_1 and the second after the total frame time T_{FT}. The modulation of the time instances allows the generation of varying decorrelated one-dimensional binary optical flow.

TABLE II
PERFORMANCE COMPARISON

	[17]	[18]	This Work
Method used	EMD model based on locust	Delay and correlate EMD	Differential optical flow imaging
Collision alert distance	63 m	$\sim$ 4 cm	$<$ 2 cm

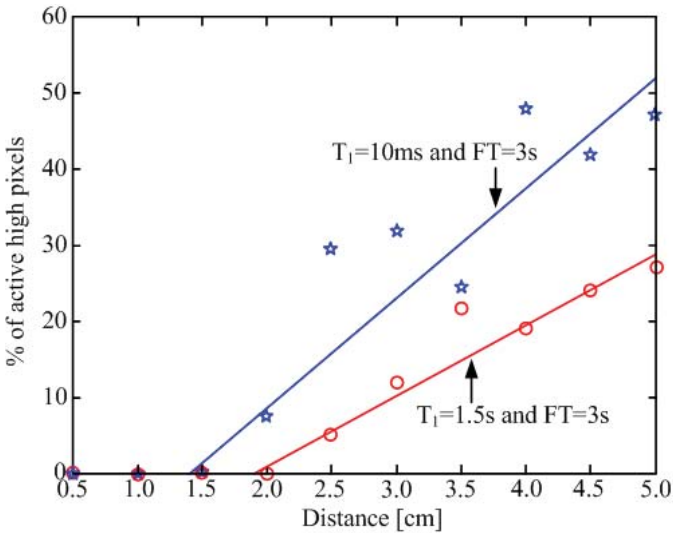

Fig. 13. Temporal differential decorrealated optical flow with approaching object.

The difference of the two temporally decorrelated optical flows is plotted in the figure 13. It can be observed that as the object moves towards the image sensor, it has a certain threshold of percentage of pixels with changed states below which the object is very near to collision. In this case the collision detection mechanism does not need to use dedicated motion processing blocks. The collision can be detected to a very good degree of reliability using the percentage of changed pixels with the varying one-dimensional differential optical flow.

Harrison [18] uses a collision detection algorithm based on the basic *EMD* model and the algorithm peaks at 230 ms for an object with a velocity of 17 cm/s. Thus the collision alert is generated at a distance of approx. 4 cm. A similar method used by [17] produces a collision detection alert at a distance of 63 m. The differential optical flow is shown to generate a collision alert for distances less than 2 cm. The performance comparison of the various algorithms are presented in Table II. For narrow path autonomous agent navigations, a collision alert for very small distance is desired. For example in applications like endoscopy, a collision alert distance of less than one cm would be ideal. The distance of collision alert can also be modulated by varying the T_1 and T_{FT}, depending on the application and situation.

Furthermore the proposed algorithm doesn't suffer from the inherent disadvantage of the accurate detection of the output peak in the EMD model: the output of the differential optical flow continues to stay low near collision allowing thresholding and thus is more stable. By modulating the differential time, it would be possible to prevent collision in very narrow paths thus helping navigation for the autonomous agents.

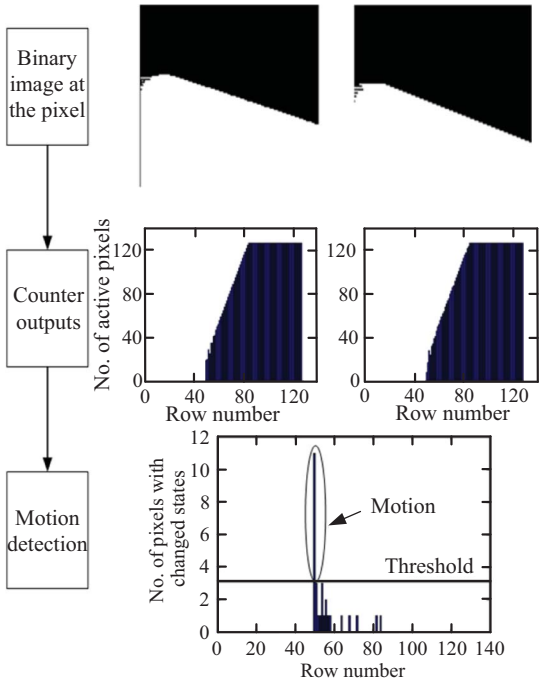

Fig. 14. Horizontal motion detection using spatially integrated binary optical flow.

B. Motion Detection in Horizontal Direction

The obtained optical flow can also be used to detect horizontal motion. The 7-bit counter counts the number of '1' in each row of the pixel for each frame. The algorithm for motion detection then compares the counter outputs to decide if there is motion. If the difference of the counters' outputs for two exposures is higher than a certain threshold, motion occurrence is flagged. For the designed sensor the brightness control voltage is the reference voltage to which the analog signal obtained after each exposure is compared.

To verify the proposed model two consecutive frames of a light source moving over the image sensor are shown in figure 4. The first image shows the light source at its initial position and the second image shows it after a slight movement. The two images look very similar, as only a very small motion was introduced. The histograms of the two images are shown in figure 14.

The subtraction of the two images results in a difference image, and the histogram of the pixels which changed states are shown at the bottom of the figure. By selecting a proper threshold, accurate detection of motion can be done.

VI. Conclusion

The compound eyes of insects are very well suited for the design of autonomous artificial biological vision systems. Inspired by them a CMOS image senor is designed operating in temporal differential mode and spatial integration of one-dimensional binary optical flow to detect motion/collision of moving objects. The binary optical flow is generated in-pixel from multiple images stored in the in-pixel memories and spatially integrated using a counter. The computations are relatively easy and experimental results show the ability to detect collision with the approaching object as near as 2 cm. This method allows the design of simple, miniaturized, low power and narrow path autonomous navigating agents.

The sensor is also able to detect polarization using a metallic wire grid patterned directly over the photodiodes using the CMOS metal layers. An extinction ratio of 7.7 was obtained for the wire grid linear polarizer. The one-dimensional binary optical flow was shown to have an angular dependence on the angle of the linear polarizer. Representing polarization information using one-dimensional binary optical flow would allow focal plane processing of polarization information and can be used in many machine vision applications. It is further observed that by increasing the number of wire grid orientations, a digital representation of the polarization very similar to the analog can be obtained.

Acknowledgment

The authors would like to thank DALSA for providing the test table to characterize the sensor, INVOMEC for helping with the fabrication of the chip, A. Mierop of DALSA, G. Meynants of CMOSIS and P. Merken for their valuable contributions to this paper.

References

[1] T. Tokuda, H. Yamada, H. Shimohata, K. Sasagawa, and J. Ohta, "Polarization-analyzing CMOS image sensor with embedded wire-grid polarizer," in *Proc. Int. Image Sens. Workshop Conf.*, 2009, pp. 313–316.

[2] M. Sarkar, D. S. Segundo, C. V. Hoof, and A. J. P. Theuwissen, "Polarization analyzing CMOS image sensor," in *Proc. Int. Symp. Circuits Syst. Conf.*, 2010, pp. 621–624.

[3] X. Zhao, A. Bermak, and F. Boussaid, "A CMOS digital pixel sensor with photopatterened micropolarizer array for real time focal plane polarization imaging," in *Proc. IEEE Biomed. Circuits Syst. Conf.*, Nov. 2008, pp. 145–148.

[4] J. Tanner and C. Mead, *An Integrated Analog Optical Motion Sensor*. New York: IEEE Press, 1986.

[5] A. Moini, A. Bouzerdoum, K. Eshraghian, A. Yakovleff, X. T. Nguyen, A. Blanksby, R. Beare, D. Abbott, and R. E. Bogner, "An insect vision based motion detection chip," *IEEE J. Solid-State Circuits*, vol. 32, no. 2, pp. 279–283, Feb. 1997.

[6] J. Tuthill and S. Johnsen, "Polarization sensitivity in the red swamp crayfish Procambarus clarkii enhances the detection of moving transparent objects," *J. Exp. Biol.*, vol. 209, pp. 1612–1616, May 2006.

[7] M. Sarkar, "A biologically inspired CMOS image sensor," Ph.D. dissertation, Tech. Univ. Delft, Delft, Netherlands, 2011.

[8] C. Anderson, P. Burt, and G. V. D. Wal, "Change detection and tracking using pyramid transformation techniques," in *Proc. Intell. Robot. Comput. Vis. Conf.*, 1985, pp. 72–78.

[9] I. Haritaoglu, L. S. Davis, and D. Harwood, "W4 who? when? where? what? a real time system for detecting and tracking people," in *Proc. Int. Conf. Autom. Face Gesture Recogn.*, 1998, pp. 222–227.

[10] J. L. Barron, D. J. Fleet, and S. S. Beauchemin, "Systems and experiment performance of optical flow techniques," *Int. J. Comput. Vis.*, vol. 12, no. 1, pp. 43–77, 1994.

[11] G. Doretto and S. Soatto, "Editable dynamic textures," in *Proc. IEEE Comput. Soc. Conf. Comput. Vis. Pattern Recogn.*, Jun. 2003, pp. 137–142.

[12] A. M. Elgammal, D. Harwood, and L. S. Davis, "Non-parametric model for background subtraction," in *Proc. IEEE Eur. Conf. Comput. Vis.*, Jul. 2000, pp. 751–767.

[13] A. Borst, "How do flies land? from behavior to neuronal circuits," *BioScience*, vol. 40, no. 4, pp. 292–299, 1990.

[14] R. A. A. Brinkworth and D. C. O'Carroll, "Robust models for optic codeing in natural scenes inspired by insect biology," *PLoS Comput. Biol.*, vol. 5, no. 11, pp. 1–14, 2009.

[15] A. Borst, "Correlation versus gradient type motion detectors: The pros and cons," *Phil. Trans. Royal Soc., B, Biol. Sci.*, vol. 362, no. 1479, pp. 369–374, 2007.
[16] W. Reichardt, "Autocorrelation, a principle for the evaluation of sensory information by the central nervous system," in *Proc. Principle Sens. Commun. Conf.*, 1961, pp. 303–317.
[17] H. Okuno and T. Yagi, "Bio-inspired real-time robot vision for collision avoidance," *J. Robot. Mechatron.*, vol. 20, no. 1, pp. 68–74, 2008.
[18] R. R. Harrison, "A biologically inspired analog IC for visual collision detection," *IEEE Trans. Circuits Syst. I, Reg. Papers*, vol. 52, no. 11, pp. 2308–2318, Nov. 2005.
[19] M. Sarkar, D. S. Segundo, C. V. Hoof, and A. J. P. Theuwissen, "Integrated polarization analyzing CMOS image sensor for real time material classification," *IEEE Sens. J.*, vol. 11, no. 8, pp. 1692–1703, Aug. 2011.
[20] V. Gruev, R. Perkins, and T. York, "CCD polarization imaging sensor with aluminum nanowire optical filters," *Opt. Exp.*, vol. 18, no. 18, pp. 19087–19094, 2010.
[21] X. Zhao, A. Bermak, F. Boussaid, and V. Chigrinov, "Liquid-crystal micropolarimeter array for visible linear and circular polarization imaging," in *Proc. Int. Symp. Circuits Syst. Conf.*, 2009, pp. 637–640.
[22] M. Sarkar, D. S. Segundo, C. V. Hoof, and A. J. P. Theuwissen, "An analog and digital representation of polarization using CMOS image sensor," in *Proc. 5th Eur. Opt. Soc. Trop. Meeting Adv. Imag. Technol.*, 2010, pp. 1–2.
[23] P. Lichtsteiner, C. Posch, and T. Delbruck, "A 128 × 128 dB IS J. Ls latency asynchronous temporal contrast vision sensor," *IEEE J. Solid State Circuits*, vol. 43, no. 2, pp. 566–576, Feb. 2008.
[24] T. Delbruck and P. Lichtsteiner, "Fast sensory motor control based on event-based hybrid neuromorphic-procedural system," in *Proc. Int. Symp. Circuits Syst. Conf.*, 2007, pp. 845–848.
[25] Z. Xiangyu and C. Shoushun, "A hybrid-readout and dynamic-resolution motion detection image sensor for object tracking," in *Proc. Int. Symp. Circuits Syst.*, 2012, pp. 1628–1631.

Mukul Sarkar (S'10–M'11) received the M.Sc. degree from the University of Technology, Aachen, Germany, in 2006, and the Ph.D. degree with research on biologically inspired CMOS image sensors from the Delft University of Technology, Delft, The Netherlands.

He was a Full Time Resident with imec, Leuven, Belgium, from 2007 to 2011. From 2003 to 2005, he was with the Philips Institute of Medical Information, Aachen, as a Research Assistant, where he was involved research on detection and analysis of biosignals. Since 2012, he has been with the Department of Electrical Engineering, Indian Institute of Technology Delhi, New Delhi, India, as an Assistant Professor. His current research interests include solid-state imaging, bioinspired vision systems, analog and digital circuit design, and machine vision.

David San Segundo Bello (M'98) received the M.Sc. degree from the Universitat Autònoma de Barcelona, Barcelona, Spain, and the Ph.D. degree with research on the design of pixel-level ADCs for hybrid X-ray detectors in collaboration with the Dutch Institute of High Energy Physics and CERN, from the University of Twente, Enschede, The Netherlands.

He was a Design Engineer with the Wireline Group, Infineon Technologies (currently Lantiq), from 2004 to 2008, where he was involved in the design of line drivers and analog to digital converters for digital subscriber line applications. Since 2008, he has been with imec, Eindhoven, The Netherlands, where he is involved in the design of electronic systems and integrated circuits for image sensors. His current research interests include image sensor systems, high-resolution data converters, and CMOS sensor readout electronics.

Chris van Hoof (M'91) received the Ph.D. degree in electrical engineering from the University of Leuven, Leuven, Belgium, in 1992, in collaboration with imec, Leuven.

He was the Head of the Detector Systems Group, in 1998, the Director of the Microsystems and Integrated Systems Department, in 2002, and the Program Director of Smart Implants, in 2007, and has been the Director of the HUMAN++ Program and the Director of Integrated Systems, since 2009, with imec, and with the Holst Centre, Eindhoven, The Netherlands. His current research interests include design, technology, and applications of body-area networks and heterogeneous integration for medical and imaging applications. Since 2000, he has been a Professor with the University of Leuven, Leuven. He has authored or co-authored over 250 papers in journals and conferences.

Albert J. P. Theuwissen (M'82–SM'95–F'02) was born in Maaseik, Belgium, on December 20, 1954. He received the M.S. and Ph.D. degrees in electrical engineering from the Catholic University of Leuven, Leuven, Belgium, in 1977 and 1983, respectively.

He was with the ESAT-Laboratory, Catholic University of Leuven, from 1977 to 1983, where he was involved in research on linear charge-coupled device image sensors. In 1983, he joined the Micro-Circuits Division, Philips Research Laboratories, Eindhoven, The Netherlands, where he was involved in research on the solid-state imaging, which resulted in the project leadership of research on SDTV- and HDTV-imagers, and he became the Department Head of Imaging Devices Division in 1991. He was a Part-Time Professor with the Delft University of Technology, Delft, The Netherlands, in 2001, where he taught courses on solid-state imaging and guided the doctoral research on CMOS image sensors. In 2002, he joined DALSA Corp. as the Chief Technology Officer, where he is the Chief Scientist after retirement. In 2007, he started his own company, Harvest Imaging, which focuses on consulting, training, teaching, and coaching on solid-state imaging technology. In 2006, he co-founded ImageSensors, Inc. (a nonprofit entity) to address the needs of the image sensor community. He has authored or co-authored over 120 technical papers in journals and conferences. He has authored a textbook entitled, *Solid-State Imaging with Charge-Coupled Devices*. He holds several patents.

Dr. Theuwissen was a recipient of the SMPTE's Fuji Gold Medal in 2008, for his contributions to the research on solid-state imaging. He was a member on the Paper Selection Committee of the International Electron Devices Meeting, in 1988, 1989, 1995, and 1996. He is a Co-Editor of the IEEE TRANSACTIONS on ELECTRON DEVICES special issues on SOLID-STATE IMAGE SENSORS in 1991, 1997, 2003, and 2009, and of the *IEEE Micro special issue on Digital Imaging* in 1998. He became an IEEE ED in 1998 and a SSCS Distinguished Lecturer in 2007. He acted as the General Chairman of the IEEE International Workshop on Charge-Coupled Devices and Advanced Image Sensors in 1997, 2003, and 2009. He is a member on the Steering Committee of the aforementioned workshop and the Founder of the Walter Kosonocky Award, which highlights the best paper on solid-state image sensors. He was a member on the Technical Committee of the European Solid-State Device Research Conference and of the European Solid-State Circuits Conference. Since 1999, he has been a member on the Technical Committee of the International Solid-State Circuits Conference for which he was the Secretary, the Vice-Chair, or the Chair of the European ISSCC Committee, and a member of the overall ISSCC Executive Committee. Recently, he was elected as the International Technical Program Chair, the Vice-Chair, and the Chair of, respectively, the ISSCC 2009 and the ISSCC 2010. He is a member on the Editorial Board of *Photonics Spectra* and a member of the International Society of Optics and Photonics.